# Reversible Electronic Charge Transfer between Au Nanoparticles and Electrochromic NiO Matrices upon Electrochemical Cycling

**ARTICLE** *in* THE JOURNAL OF PHYSICAL CHEMISTRY C · OCTOBER 2007

Impact Factor: 4.77 · DOI: 10.1021/jp0758162



**2 AUTHORS:**

Fabio Furlan Ferreira
Universidade Federal do ABC (UFABC)
**70** PUBLICATIONS **538** CITATIONS
SEE PROFILE

E. Avendaño
University of Costa Rica
**27** PUBLICATIONS **1,271** CITATIONS
SEE PROFILE

Article

# Reversible Electronic Charge Transfer between Au Nanoparticles and Electrochromic NiO Matrices upon Electrochemical Cycling

Fabio Furlan Ferreira, and Esteban Avendao

*J. Phys. Chem. C*, **2007**, 111 (44), 16608-16612 • DOI: 10.1021/jp0758162

# Reversible Electronic Charge Transfer between Au Nanoparticles and Electrochromic NiO Matrices upon Electrochemical Cycling

**Fabio Furlan Ferreira* and Esteban Avendaño†**

*Laboratório Nacional de Luz Síncrotron (LNLS), Caixa Postal 6192, CEP 13083-970, Campinas, SP, Brazil*

*Received: July 24, 2007; In Final Form: August 29, 2007*

Cyclic voltammetry measurements and XANES spectra of hydrated NiO films with metallic Au nanoparticles embedded in them showed an electrochemical activity that modified their overall properties when incorporated in a galvanic cell. With respect to the electrochromic properties, Au nanoparticles played an important role in the final coloration state of the films by means of charge transfer between the gold oxide at the surface of metallic Au nanoparticles and the $NiO_xH_y$ matrix. The results are consistent with the spectral changes seen in the coloration efficiency of films with approximately the same amount of electrochromic material (i.e., $NiO_xH_y$). In addition, the incorporation of Au nanoparticles produced an increase of about 50% in the charge capacity of the films, a value that is expected to be a function of the average diameter of the Au nanoparticles. Such increments in charge capacity open up the possibility of using this kind of system in applications that require optimized charge capacity, like batteries. The present work was carried out to show the existence of an electronic charge transfer between Au nanoparticles (NPs) and the electrochromic NiO matrix.

## Introduction

Reversible charge storage in anodic hydrated NiO ($NiO_xH_y$) films has been of great concern during the last few years, especially in applications such as electrochromic (EC) devices, which show a persistent and reversible optical modulation when, by means of an external applied electric field, ions are electrochemically intercalated in their structure,[1] and batteries, in which the electrical energy is generated by conversion of chemical energy via redox reactions at the anode and cathode.[2] The subject of these classes of research is of particular interest in today's main technologies related to energy saving and energy-storage devices.

Electrochromic oxide thin films may be employed in optical devices of different types like displays, smart windows, light shutters, variable reflectance mirrors, and gas sensors, among others.[3] Nanoparticles (NPs) embedded in electrochromic matrices have been attracting the attention of the scientific community because of the possibility of combining the optical modulation of the matrix with the selective absorption of metallic NPs embedded in it.[4] The main interest in these systems relies on the possibilities of tailoring their optical and electrical properties over a wide range of values. The potential application in electrochromic devices is centered on the feasibility of obtaining reflected and/or transmitted colors different from the original tint in inorganic compounds. For example, the growth of anodic colored $Au-NiO_x$ (blue, violet, red) films, different from pure $NiO_x$ (transparent, dark-gray), makes possible their assemblage with the cathodic $WO_{3-x}$ in EC windows, producing different mixtures of colors for facades in architectural applications.

Theoretical studies using the Maxwell Garnett effective medium theory have predicted that gold NPs embedded in electrochromic NiO films present selective absorption in the visible region.[4,5] In the literature, metal-cathodic materials are described but, surprisingly, there are only a few reports on the metal-anodic ones, only for use in gas sensors.[6−8] Some cathodic systems have been tested already, such as $Au-WO_3$,[9,10] $Au-MoO_3$,[11,12] and $Au-V_2O_5$.[13] Our previous theoretical studies making use of the Maxwell Garnett effective medium theory fine-tune the optical properties for the $Au-NiO_x$ system.[5] The final color of the composite film depends on the size of the Au NPs, their aggregation state (shape), and their interaction with the matrix, that is, the local dielectric environment.[14]

In order to understand the correlation between Au NPs and the $NiO_xH_y$ matrix concerning its morphology, structural properties, charge capacity, and electronic structure in the as-grown, maximum bleached, and colored states, we performed measurements of cyclic voltammetry, spectral transmittance and reflectance, electron microscopy, and X-ray absorption spectroscopy.

## Experimental Section

Electrochromic nickel oxide ($NiO_x$) and composite gold−nickel oxide ($Au-NiO_x$) thin films were deposited by reactive DC sputtering using a deposition system based on a Balzers Sputtron unit, alternating 12 NiO layers with 11 discontinuous Au layers. The targets were 6-cm-diameter plates of Au and Ni with 99.95% purity. Sputtering was conducted in an $Ar + O_2$ plasma. The gases were 99.995% pure. The substrates were $In_2O_3$:Sn (ITO)-covered Corning glass plates, prior cleaned in an oxygen plasma, positioned 27 cm from the targets. The working sputter pressure was 30 mTorr, and the sputtering power was kept at 1.5 kW. The samples were deposited at room temperature. As-deposited samples were characterized by optical and cyclic voltammetry (CV) measurements. Samples with a greater amount of gold were characterized by X-ray absorption (XAS) measurements. These samples were postannealed (at 200 °C for $t = 10$ s and 400 °C for $t = 20$ s) using a rapid thermal annealing (RTA) system in order to obtain larger crystallite sizes. No differences in the electrochemical and

* Corresponding author. E-mail: furlan@lnls.br. Phone: +55 19 3512-1043. Fax: +55 19 3512-1004.

† Present address: Chromogenics Sweden AB.

10.1021/jp0758162 CCC: $37.00 
Published on Web 10/11/2007

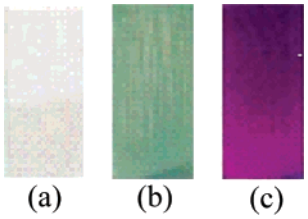


**Figure 1.** Color variations of the composite films, after several cycles of charge/discharge, as a function of the number of multilayer-deposited (a) pure $NiO_xH_y$, (b) 2-$NiO_xH_y$/1-Au multilayers, and (c) 9-$NiO_xH_y$/8-Au multilayers. The film thicknesses are 53, 60, and 63 nm, respectively.

optical response between the sets of samples were found. Deposition rates were obtained from sputtering time and film thicknesses were recorded by surface profilometry (DECTACK 3ST VECO) across a step made in the films. Typical deposition rates were 0.1 for Au and 0.3 nm $s^{-1}$ for NiO, and film thicknesses were about 130 nm.

Ex situ optical and voltammetric measurements were performed on the films using a double-beam Lambda 9 spectrophotometer (Perking Elmer) and an AUTOLAB potentiostat, respectively. The electrochemical cycling was made using a three-electrode cell in a 1.0 M KOH solution. A Pt counter electrode and an Ag/AgCl (1.0 M) reference electrode were used. The scanning rate was 10 $mVs^{-1}$, and the spectra were taken after 50 cycles in the colored and bleached states.

Transmission electron microscopy work has been performed with the JEM-3010 ARP microscope of the LME/LNLS, Campinas, Brazil and was used to study both the morphology and the size of Au NPS of the samples.

All experiments using synchrotron radiation facilities were performed ex situ after 50 voltammetry cycles in the as-grown, colored, and bleached states, to ensure charge stabilization, at the Brazilian Synchrotron Light Laboratory (LNLS - Campinas, Brazil).

X-ray absorption measurements (XAS) were recorded in fluorescence mode at the X-ray absorption spectroscopy (D04B − XAFS1) beamline.[15] The spectra were recorded at room temperature with a multielement solid-state Ge detector at the Ni K (8333 eV) and Au $L_{III}$ edges (11919 eV). The monochromator was a channel-cut Si(111) ($2d = 6.271$ Å) crystal. The calibration was carried out using the first inflection point of the spectra of Ni and Au foils as references. Each spectrum corresponds to an average over three independent scans.

## Results and Discussion

The number of multilayers deposited changes the way that Au nanoparticles aggregate, and so their size, thus leading the material to present a different selective absorption characteristic, as can be seen in Figure 1. After several charge/discharge electrochemical cycles in a base solution (1.0 M KOH electrolyte), the color of the composite material changed from gold-brown to green, blue, violet, and so forth, when reaching the stabilization charge. Figure 1a shows the color of the pure $NiO_xH_y$ film after several cycles of charge/discharge. It changes its characteristic light-gray color (charged) to dark-brown (discharged). When gold was added, the film changed from its characteristic color to green (Figure 1b) and violet (Figure 1c) also after several cycles of charge/discharge. It should be mentioned that the as-grown materials do not present such colors. The films shown in Figure 1b and c were deposited as having two $NiO_x$ layers and one discontinuous Au layer and nine $NiO_x$ layers and eight discontinuous Au layers, respectively.

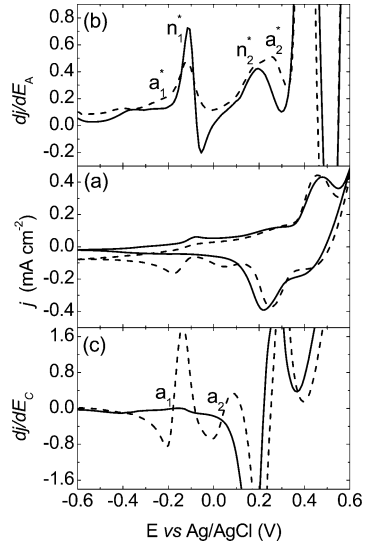


**Figure 2.** (a) Cyclic voltammetry of the $NiO_xH_y$ (solid line) and Au−$NiO_xH_y$ (dashed line) films after 50 scans. A three-electrode configuration was used in a 1.0 M KOH solution. The intercalated charge during the cathodic cycle (sample in the bleached state) is 11.9 and 16.8 mC $cm^{-2}$, respectively, for the $NiO_xH_y$ and Au−$NiO_xH_y$ films. Derivatives for the half-cycle in the (b) anodic and (c) cathodic intercalation with respect to the potential, d$j$/d$E_i$.

Cyclic voltammetries of nickel and gold−nickel oxides are shown in Figure 2a with their respective half-cycle derivatives in the anodic and cathodic cycles with respect to the potential, d$j$/d$E_i$, with $i$ being A (anodic, in Figure 2b) and C (cathodic, in Figure 2c). The films presented a good electrochemical switching as well as the activity of the Au NPs embedded in the hydrated NiO matrix. The reaction mechanism scheme for hydrated nickel oxide films has been reviewed extensively in Avendaño et al.[16] The letters in Figure 2b and c, $n_i$ and $a_i$, correspond to the features ascribed to the hydrated nickel oxide and gold oxide, respectively. The description of the $n_i$ features in nickel oxide is described in ref 16. The extra features observed in the cyclic voltammogram of the Au−$NiO_xH_y$ sample illustrate the electron exchange of $Au^{1+}$ in the pair $n_1$ and $Au^{3+}$ in the pair $n_2$.[17] The detected activity has been explained as the result of activation of the first layers in gold electrodes cycled in base solutions.[18,19]

The incorporation of gold NPs into the matrix produced an increase of the charge capacity, $\Delta Q_{\text{charge capacity}}$, which was calculated taking the cathodic half-cycle (bleaching). It is important to notice that the calculus of the charge capacity was corrected by the $iR$ drop,[20] that is, the potential drop between the counter and reference electrodes, and extreme care was taken in order to not produce oxygen or hydrogen evolution during the electrochemical cycling. The calculated values were 11.9 and 16.8 mC $cm^{-2}$ for the $NiO_xH_y$ and the composite Au−$NiO_xH_y$, respectively. An increase of approximately 50% could be observed in the charge capacity of the gold-embedded film with respect to the pure $NiO_xH_y$ film. This is an important result once it opens up the possibility of using this kind of system in applications that require optimized charge capacity, such as batteries. The total amount of gold deposited into the samples, estimated from the deposition rates, was estimated to be about 20−25 wt %. It is also important to notice that similar results were obtained in a previous investigation.[21]

High-resolution transmission electron microscopy (HRTEM) images gave evidence of the formation of Au NPs as having about 10 nm, as shown in Figure 3. An electron beam with a spot size of about 10 nm, in order to perform qualitative nano

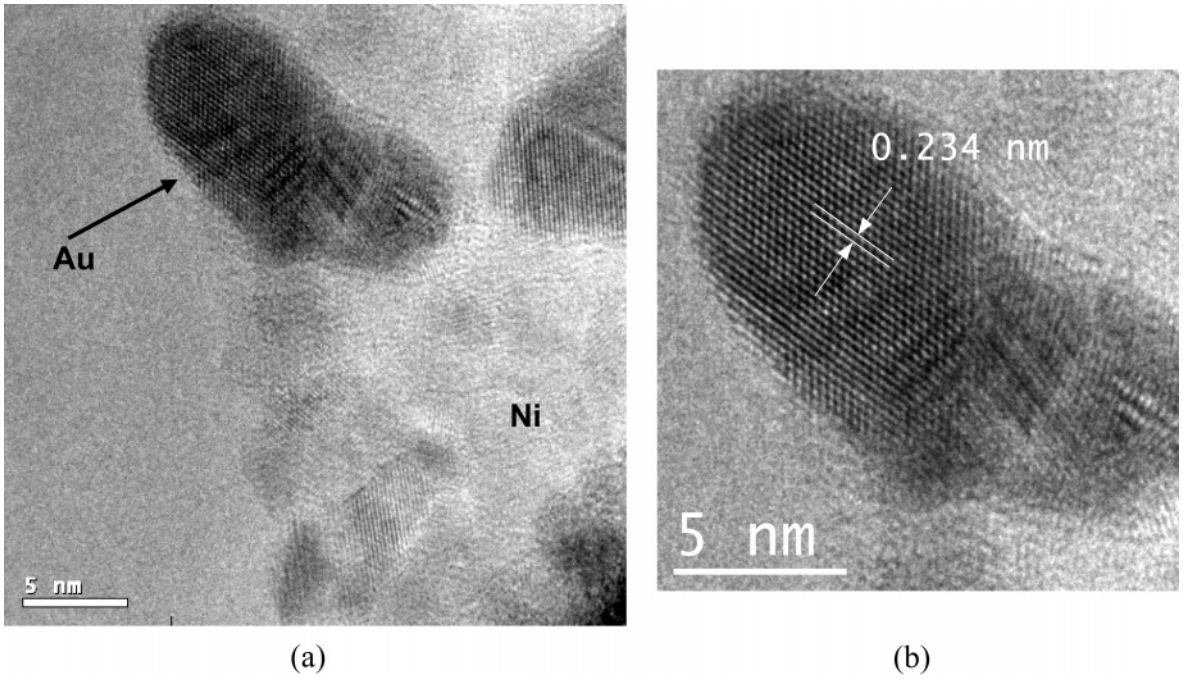


**Figure 3.** (a) HRTEM image of gold NPs embedded in an electrochromic nickel oxide matrix. Nano EDX was used in order to identify the regions indicated by arrows. (b) Details of the Au nanoparticle.

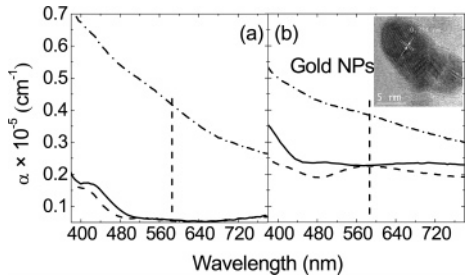


**Figure 4.** Absorption coefficients of the (a) $NiO_xH_y$ and (b) Au−$NiO_xH_y$ films after 50 CV cycles in a 1.0 M KOH solution for the as-grown (solid line), bleached (dashed line), and colored (dash-dotted line) states.

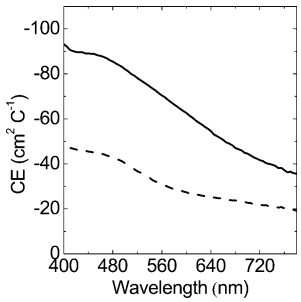


**Figure 5.** Coloration efficiency (CE) of the $NiO_xH_y$ (solid line) and Au−$NiO_xH_y$ (dashed line) films after 50 electrochemical cycles. A three-electrode configuration was used in a 1.0 M KOH solution.

energy-dispersive X-ray spectrometry (EDX) analyses, was used. Au NPs as well as NiO regions could be identified and are also indicated in Figure 3. The measured distance between two parallel planes, equal to 0.234 nm, gives indication of the {1,1,1} family planes seen close to a [0,1,1] zone axis. This value is in accordance with the indexed (111) crystallographic plane of metallic Au.[22] When Au was added to the deposition process, there was an increase of the surface roughness, observed by field-emission gun scanning electron microscopy (not shown).

The broad peak at approximately 580 nm (indicated by a dashed line) in the absorption coefficient for the gold−nickel oxide film in Figure 4 is indicative of the formation of NPs inside the films. Our results using Maxwell Garnett effective medium theory predict such a response in the absorption for particles with an average size of about 5−10 nm.[4] The confirmation of the distribution was done by HRTEM (Figure 3), and the identification of the particles was performed by nano EDX.

In situ spectral transmittance, $T(\lambda)$, and reflectance, $R(\lambda)$, data were recorded for the colored and bleached states and, thus, combining optical and electrochemical measurements, the spectral coloration efficiency (CE) was obtained from a standard relation.[23] The calculated coloration efficiency at 580 nm is −66 and −29 $cm^2\ C^{-1}$, respectively, as shown in Figure 5, for the hydrated nickel oxide and gold NPs embedded in hydrated nickel oxide in films with roughly the same equivalent content of the electrochromic material. The effect of gold in the coloration efficiency (CE) produced a diminution in the contrast between the gold-containing and pure $NiO_xH_y$ film. Such differences in the CE suggest that the gold electrochemical activity charge compensates the electron transfer in the hydrated nickel oxide, indicating that during the oxidation of the gold surface into $Au^{3+}$ species some of the electrons transform the $Ni^{3+}$ site into a $Ni^{2+}$ site diminishing the absorption in the colored state. This result is later confirmed by XANES. It is important to clarify that the gold activity is associated with the atoms placed at the surface of the NPs, thus representing much less active material when compared with the electrochromic matrix (i.e., hydrated NiO) itself. In this way, even taking into account that the oxidation and reduction of gold is a two-electron process and the electrochromic reaction of the matrix is mainly a one-electron process with a small fraction of a two-electron process, there is a fraction of charge that is not taking part in the coloration process.

Figure 6a shows the X-ray absorption near edge structure (XANES) spectra at the Au $L_{III}$ edge of the Au−$NiO_xH_y$, in different coloration states, and the $AuO_x$ samples together with that of Au foil, taken as reference material. The XANES spectra were plotted with respect to $E - E_0$, $E_0$ being defined as the position of the first inflection point. The spectrum of $Au^0$ from

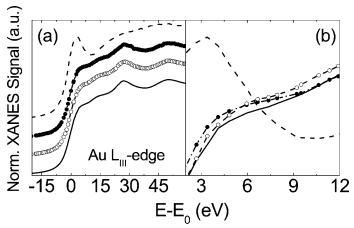


**Figure 6.** (a) Normalized (and shifted, for better visualization) XANES spectra, taken at the Au $L_{II}$ edge, when the electrochromic Au−$NiO_xH_y$ film is in the bleached (white circle + solid line) and colored (black circle + solid line) states after 50 cycles in a 1.0 M KOH solution together with those of an $AuO_x$ (dashed line) film and of Au (solid line) foil. (b) Details of the characteristic normalized white line region, without shifting the spectra.

gold foil presents a shoulder at about 15 eV above the absorption edge (located at 0 eV and assumed as the edge inflection point) and intense peaks at ∼27 and 50 eV. Those peaks emerge from only *fcc* structures ordered up to the third shell.[24−26] The first resonance at the edge is known as a white line. The white line in the spectrum of $Au^0$ from gold foil arise from 2p(Au) → 5d(Au) dipole transitions, the intensity of which is very strong for most transition metals with a partially filled d band and is related to the unoccupied densities of d states (d-hole counts).[26] Although the 5*d* orbitals in Au atoms are nominally full, because of s−p−d hybridization, a small white line can still be detected in the XANES of bulk Au.[27,28] The area under the white line can thus be utilized to study the d-charge (hole) redistribution in various gold samples.[27,28] As can be seen in Figure 6b, there is a decrease of the white line intensity with an electron excess. The dashed-line spectrum corresponds to an unknown oxidized sample with a shape similar to that presented by an $Au_2O_3$ sample.[29,30] The sample in the colored state is found to be more oxidized than that in the bleached state, both of them being slightly more oxidized when compared to the bulk Au. The intensity of the white line varies depending on the size of the cluster,[31] which can be related to the existence of inequivalent sites in small clusters, meaning that a size effect can be observed directly on the white line. According to the literature[31] at least two physical phenomena can affect the intensity of the white line: the size of the cluster, which can be considered as an intrinsic effect, and a charge transfer between the cluster and the support, which can be considered as an extrinsic one. This latter effect can be evidenced in more detail in Figure 7d, which illustrates the intensity of the white line, in different coloration states, of the composite Au−$NiO_xH_y$ film, measured on the Ni K edge. Different from what was seen in Figure 6b, the white line is now more intense in the bleached state of the Au−$NiO_xH_y$ film. This is direct evidence of the charge transfer between the Au NPs and the NiO matrix, which explains the smaller coloration efficiency in the composite film (CE at 580 nm is −29 vs −66 $cm^2\ C^{-1}$ in the pure $NiO_xH_y$ film).

XANES spectra taken at the Ni K edge are shown in Figure 7a. A difference between the *c*-NiO reference and $NiO_xH_y$ film is present in the intensity of the preedge peak around $E - E_0 = -12$ eV (not shown) and in the characteristic shoulder located above the preedge peak, around $E - E_0 = -3$ eV. The preedge peak is associated with a transition from the 1s(Ni) → 3d(Ni) states mixed with the 2p(O) states.[32] The origin of the preedge peak is due to an increase of the oxygen−nickel charge-transfer energy accompanied by a reduction of the amount of ground-state configurations with holes in the 2p(O) states, explained by the Zaanen−Sawatzky−Allen model.[33] In the case of Au−$NiO_xH_y$, such behavior is also observed. However, the film in the colored state presents a more intense preedge feature than

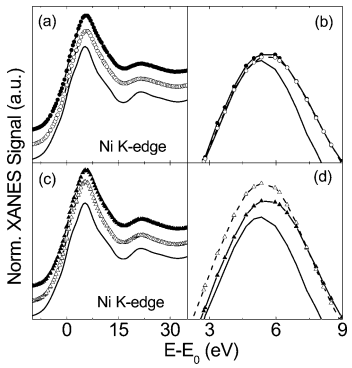


**Figure 7.** Normalized (and shifted, for better visualization) XANES spectra, taken at the Ni K edge, when the electrochromic (a) $NiO_xH_y$ (bleached: white circle + solid line; colored: black circle + solid line) and (c) Au−$NiO_xH_y$ (bleached: white triangle + solid line; colored: black triangle + solid line) films are in the bleached and colored states after 50 cycles in a 1.0 M KOH solution together with that of a c-NiO (black solid line) film. In d and d, we presented the details of the normalized white line (without shifting the spectra) for the spectra plotted in a and c, respectively.

the film in the bleached state, meaning that the presence of oxidized gold increases the amount of ground-state configurations in $NiO_xH_y$ by means of charge-transferred electrons.

The increase of the white line intensity for the $NiO_xH_y$ film in the colored state, depicted in Figure 7b, is expected because of the changes in the valence from $Ni^{2+}$ to $Ni^{3+}$, being related to transitions from the bleached to the colored state, respectively. This change in valence results in modifications of the Ni−O local environment that, in turn, produces a decrease of the preedge peak intensity in films when compared to *c*-NiO (not shown). This effect is associated with the fact that the Ni−O bonding becomes less covalent. In the case of the Au−$NiO_xH_y$ film, shown in Figure 7d, the white line intensity has behavior opposite of that observed in $NiO_xH_y$ (Figure 7b). An overall increase of the white line of the Au−$NiO_xH_y$ film (in the colored and bleached states) with respect to the $NiO_xH_y$ film (also in the colored and bleached state) and *c*-NiO gives direct evidence of the charge transfer between the Au NPs to the NiO matrix. These changes explain the smaller coloration efficiency seen in the Au−$NiO_xH_y$ film because of the diminishing of the $Ni^{3+}$ sites during the coloration process.

## Conclusions

In summary, we have shown that the sputter-deposited composite gold−nickel film presented a good electrochemical switching and an increase of about 50% in the charge capacity with respect to the NiO matrix alone. The addition of gold promoted an increase of the surface roughness with respect to the pure NiO matrix and the size of Au nanoparticles was estimated to be about 10 nm, as determined by electron microscopy images. The effect of gold in the coloration efficiency produced a diminution in the contrast when compared with the $NiO_xH_y$ film. To our knowledge, this is the first time that XANES measurements were performed in this kind of system and showed that the gold nanoparticles are found to be oxidized, independent of the coloration state, being more oxidized in the colored (anodic) state. The measurements showed that the $NiO_xH_y$ film changed from $Ni^{2+}$ to $Ni^{3+}$ during electrochemical cycling, corresponding to the bleached and colored states, respectively. In the case of the Au−$NiO_xH_y$ film, the results indicated that a charge transfer occurred between the Au NPs and the NiO matrix, thus diminishing the $Ni^{3+}$ sites during the anodic coloration. Such changes explain the smaller

coloration efficiency (contrast between the colored and bleached states per charge unity) in the $Au-NiO_xH_y$ film because of the diminishing of the $Ni^{3+}$ sites during the coloration process.

Our results showed that gold NPs can be used as an electrochromic material under certain conditions that extend their usual application and extend the list of materials that, in a controlled and stabilized way, can be induced to present changes of color by oxidation and reduction processes; in this case, from metallic gold to a semitransparent dark-brown color.

**Acknowledgment.** We thank the LNLS for beam time and infrastructure, the LME/LNLS for technical support during electron microscopy work, Dr. D. Zanchet for the TEM images, MSc. A. Gobbi for the RTA processing, and the Solid-State Physics Department at the Uppsala University, Sweden, through the Angstrom Laboratory for the cyclic voltammetry and in situ and ex situ spectral transmittance and reflectance measurements.

## References and Notes

(1) Granqvist, C. G., *Handbook of Inorganic Electrochromic Materials*; Elsevier: Amsterdam, 1995, reprinted 2002.
(2) Winter, M.; Brodd, R. J. *Chem. Rev.* **2004**, *104*, 4245.
(3) Azens, A.; Avendaño, E.; Backholm, J.; Berggren, L.; Gustavsson, G.; Karmhag, R.; Niklasson, G. A.; Roos, A.; Granqvist, C. G. *Mater. Sci. Eng., B* **2005**, *119*, 214.
(4) Ferreira, F. F.; Fantini, M. C. A. *J. Phys. D: Appl. Phys.* **2003**, *36*, 2386.
(5) Fantini, M. C. A.; Ferreira, F. F.; Gorenstein, A. *Solid State Ionics* **2002**, *152−153*, 867.
(6) Ando, M.; Kobayashi, T.; Haruta, M. *Sens. Actuators, B* **1995**, *25*, 851.
(7) Ando, M.; Kobayashi, T.; Iijima, S.; Haruta, M. *J. Mater. Chem.* **1997**, *7*, 1779.
(8) Mattei, G.; Mazzoldi, P.; Post, M. L.; Buso, D.; Guglielmi, M.; Martucci, A. *Adv. Mater.* **2007**, *19*, 561.
(9) Sichel, E. K.; Gittleman, J. I.; Zelez, J. *Appl. Phys. Lett.* **1977**, *31*, 109.
(10) He, T.; Ma, Y.; Cao, Y.; Yang, W. S; Yao, J. N. *J. Electroanal. Chem.* **2001**, *514*, 129.
(11) Yao, J. N.; Yang, Y. A.; Loo, B. H. *J. Phys. Chem. B* **1998**, *102*, 1856.
(12) He, T.; Ma, Y.; Cao, Y.; Yin, Y. H.; Yang, W. S.; Yao, J. N. *Appl. Surf. Sci.* **2001**, *180*, 336.
(13) Nagase, K.; Shimizu, Y.; Miura, N.; Yamazoe, N. *Appl. Phys. Lett.* **1994**, *64*, 1059.
(14) Kreibig, U.; Vollmer, M. *Optical Properties of Metal Clusters*; Springer: Berlin, 1995.
(15) Tolentino, H. C. N.; Ramos, A. Y.; Alves, M. C. M.; Barrea, R. A.; Tamura, E.; Cezar, J. C.; Watanabe, N. *J. Synchrotron Rad.* **2001**, *8*, 1040.
(16) Avendaño, E.; Azens, A.; Niklasson, G. A.; Granqvist, C. G. *J. Electrochem. Soc.* **2005**, *152*, F203.
(17) Sadik, O. A.; Xu, H. W.; Sargent, A. *J. Electroanal. Chem.* **2005**, *583*, 167.
(18) Juodkazis, K.; Juodkazyte, J.; Šebeka, B.; Lukinskas, A. *Electrochem. Commun.* **1999**, *1*, 315.
(19) Kirk, D. W.; Foulkes, F. R.; Graydon, W. F. *J. Electrochem. Soc.* **1980**, *127*, 1962.
(20) Hamann, C. H.; Hamnett, A.; Vielstich, W. *Electrochemistry*; Wiley-VCH: Weinheim, 1998; p 234.
(21) Ferreira, F. F.; Fantini, M. C. A. *Solid State Ionics* **2004**, *175*, 517.
(22) Joint Committee on Powder Diffraction Standards, (ICDD Powder Diffraction File-2, Swarthmore, PA, 2001) card file 04-0784.
(23) Azens, A.; Talledo, A.; Andersson, A. M.; Niklasson, G. A.; Stjerna, B.; Granqvist, C. G. *Proc. Soc. Photo-Opt. Instrum. Eng.* **1992**, *1728*, 103.
(24) Greaves, G. N.; Durham, P. J.; Diakun, G.; Quinn, P. *Nature* **1981**, *294*, 139.
(25) Balerna, A.; Bernieri, E.; Picozzi, P.; Reale, A.; Santucci, S.; Burattini, E.; Mobilio, S. *Phys. Rev. B* **1985**, *31*, 5058.
(26) Zhang, P.; Sham, T. K. *Appl. Phys. Lett.* **2002**, *81*, 736.
(27) Lytle, F. W. *Ber. Bunsen-Ges. Phys. Chem. Chem. Phys.* **1987**, *91*, 1251.
(28) Mattheiss, L. F.; Dietz, R. E. *Phys. Rev. B* **1980**, *22*, 1663.
(29) Weiher, N.; Willneff, E. A.; Figulla-Kroschel, C.; Jansen, M.; Schroeder, S. L. M. *Solid State Commun.* **2003**, *125*, 317.
(30) Weiher, N.; Bus, E.; Delannoy, L.; Louis, C.; Ramaker, D. E.; Miller, J. T.; van Bokhoven, J. A. *J. Catal.* **2006**, *240*, 100.
(31) Bazin, D.; Sayers, D.; Rehr, J. J.; Mottet, C. *J. Phys. Chem. B* **1997**, *101*, 5332.
(32) Kuzmin, A.; Purans, J.; Rodionov, A. *J. Phys.: Condens. Matter* **1997**, *9*, 6979.
(33) Zaanen, J., Sawatzky, G. A.; Allen, J. W. *Phys. Rev. Lett.* **1985**, *55*, 418.